samples were degassed by the freeze–thaw method and then sealed.

Moscau, Spectrospin AG, Fällanden, for ¹H COSY and NOESY spectra of **3a**.

Photoinduced Hydrometalation and Hydrogenation of Activated Olefins with Molybdenum and Tungsten Dihydrides (Cp₂MH₂)

J. J. Ko, T. M. Bockman, and J. K. Kochi*

Department of Chemistry, University of Houston, Houston, Texas 77204-5641
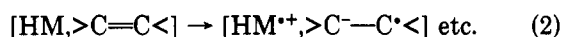
Received November 14, 1989

The early-transition-metal hydrides Cp₂MoH₂, Cp₂WH₂, and Cp₂ReH rapidly form a series of electron donor–acceptor (EDA) complexes with various activated olefins as shown by the spontaneous appearance of vivid colors, the absorption energies of which correlate with the electron affinity of the olefinic acceptor and the oxidation (ionization) potential of the hydridometal donor in accord with Mulliken theory. Deliberate excitation of the charge-transfer absorption band leads to the quantitative hydrometalation of fumaronitrile by Cp₂MoH₂ at 25 °C, and the structure of the σ hydrido alkyl adduct Cp₂Mo(CHCNCH₂CN)H (I) has been established by X-ray crystallography. (space group $P2_1$, monoclinic, with $a = 8.090$ (3) Å, $b = 10.282$ (4) Å, $c = 8.316$ (3) Å, $\beta = 116.92$ (3)°, $V = 617$ Å³, $Z = 2$, $R = 0.028$, $R_w = 0.028$ for 1802 reflections with $I > 3\sigma$ having $2\theta \le 60°$). Under the same photochemical conditions, the tungsten analogue Cp₂WH₂ effects quantitative hydrogenation and leads to succinonitrile together with the olefinic π-adducts to tungstenocene in high yields. (In both cases, the thermal (dark) processes are nonexistent.) The charge-transfer mechanism for olefin hydrometalation and hydrogenation stemming from charge separation in the EDA complex (i.e. [Cp₂MH₂⁺, >C⁻–C⁻<]) is delineated in terms of the one-electron-oxidation potential $E°_{ox}$ of the hydridometal species and the subsequent facile proton transfer from the labile cation radical Cp₂MH₂⁺ (M = Mo, W) to the acceptor moiety. The close similarity of the photoinduced process for olefin hydrometalation and hydrogenation of various activated olefins with those effected thermally at higher temperatures is discussed.

Introduction

Metal catalysis of olefin and arene hydrogenation is critically dependent on hydridometal (HM) intermediates.[1] Indeed, the separate isolation of various hydridometal complexes and their direct addition to unsaturated centers represent a viable procedure for the preparation of different types of hydrocarbyl derivatives.[2-6] The mechanism of the activation process leading to reactive intermediates in such hydrometalations is less clear. Thus, the relevance of intermediate free radicals was initially suggested on the basis of stereochemistry and relative reactivities[7] and later confirmed by EPR studies.[8] Observation of CIDNP has led to radical-pair mechanisms that stem from an overall

hydrogen atom transfer to olefinic substrates.[9-11] Although the prior ligation of substrate to HM has been established in some cases,[12] it is noteworthy that CIDNP has so far been reported only in those systems for which there is no evidence of precoordination. In the latter case, the mechanistic basis for the intermolecular interactions leading to hydrogen atom transfer from the hydridometal intermediate to the substrate is lacking. Thus, the report of transient charge-transfer (CT) absorption bands during hydrometalations with tungsten and molybdenum hydrides is particularly interesting.[13] Since such absorption bands are diagnostic of electron donor–acceptor (EDA) precursor complexes, as in eq 1 (Scheme I),[14,15] the charge-transfer

Scheme I

$$HM + {>}C{=}C{<} \rightleftharpoons [HM,{>}C{=}C{<}] \qquad (1)$$

$$[HM,{>}C{=}C{<}] \rightarrow [HM^{\cdot+},{>}C^{-}{-}C^{\cdot}{<}] \text{ etc.} \qquad (2)$$

(1) James, B. R. *Homogeneous Hydrogenation*; Wiley: New York, 1973; *Adv. Organomet. Chem.* 1979, *17*, 319.

(2) (a) Muetterties, E. L., Ed. *Transition Metal Hydrides*; Dekker: New York, 1971. (b) Wailes, P. C.; Weigold, H.; Bell, A. P. *J. Organomet. Chem.* 1971, *27*, 373. (c) Miyake, A.; Kondo, H. *Angew. Chem., Int. Ed. Engl.* 1968, *7*, 631. (d) Mabbott, D. J.; Maitlis, P. M. *J. Chem. Soc., Dalton Trans* 1976, 2156.

(3) (a) Clark, H. C.; Kurosawa, H. *Inorg. Chem.* 1972, *11*, 1275. (b) Clark, H. C.; Jablonski, C. R. *Inorg. Chem.* 1974, *13*, 2213.

(4) (a) Thomas, K.; Osborn, J. A.; Powell, A. R.; Wilkinson, G. *J. Chem. Soc. A* 1968, 1801. (b) Werner, H.; Feser, R. *Angew. Chem., Int. Ed. Engl.* 1979, *18*, 157.

(5) (a) Booth, B. L.; Haszeldine, R. N.; Mitchell, P. R. *J. Organomet. Chem.* 1970, *21*, 203. (b) Schrauzer, G. N. *Angew. Chem., Int. Ed. Engl.* 1976, *15*, 417. (c) Linn, D. E., Jr.; Halpern, J. *J. Am. Chem. Soc.* 1987, *109*, 2969. (d) Ungvary, F.; Markó, L. *Organometallics* 1986, *5*, 2341.

(6) (a) Ito, T.; Tosaka, H.; Yoshida, S.; Mita, K.; Yamamoto, A. *Organometallics* 1986, *5*, 735. (b) Herberich, G. E.; Barlage, W. *Organometallics* 1987, *6*, 1924. (c) Herberich, G. E.; Mayer, H. *J. Organomet. Chem.* 1988, *347*, 93. (d) Amaudrut, J.; Leblanc, J. C.; Moise, C.; Sala-Pala, J. *J. Organomet. Chem.* 1985, *295*, 167. (e) Herberich, G. E.; Hessner, B.; Okuda, J. *J. Organomet. Chem.* 1983, *254*, 317.

(7) Feder, H. M.; Halpern, J. *J. Am. Chem. Soc.* 1975, *97*, 7186.

(8) Clark, H. C.; Ferguson, G.; Goel, A. B.; Janzen, E. G.; Ruegger, H.; Siew, P. Y.; Wong, C. S. *J. Am. Chem. Soc.* 1986, *108*, 6961.

(9) (a) Sweany, R. L.; Halpern, J. *J. Am. Chem. Soc.* 1977, *99*, 8335. (b) Nalesnik, T. E.; Orchin, M. *Organometallics* 1982, *1*, 222. (c) Nalesnik, T. E.; Freudenberger, J. H.; Orchin, M. *J. Mol. Catal.* 1982, *16*, 43.

(10) (a) Bockman, T. M.; Garst, J. F.; King, R. B.; Markó, L.; Ungvary, F. *J. Organomet. Chem.* 1985, *279*, 165. (b) Shackleton, T. A.; Baird, M. C. *Organometallics* 1989, *8*, 2225. (c) Connolly, J. W. *Organometallics* 1984, *3*, 1333.

(11) See, however: Eisenschmid, T. C.; Kirss, R. U.; Deutsch, P. P.; Hommeltoft, S. I.; Eisenberg, R.; Bargon, J.; Lawler, R. G.; Balch, A. L. *J. Am. Chem. Soc.* 1987, *109*, 8089.

(12) (a) Landis, C. R.; Halpern, J. *J. Am. Chem. Soc.* 1987, *109*, 1746. (b) Roe, D. C. *J. Am. Chem. Soc.* 1983, *105*, 7770. (c) Doherty, N. M.; Bercaw, J. E. *J. Am. Chem. Soc.* 1985, *107*, 2670. (d) See also: Byrne, J. W.; Blaser, H. U.; Osborn, J. A. *J. Am. Chem. Soc.* 1975, *97*, 3871.

(13) (a) Nakamura, A.; Otsuka, S. *J. Am. Chem. Soc.* 1973, *95*, 7262. (b) Nakamura, A.; Otsuka, S. *Bull. Chem. Soc. Jpn.* 1976, *49*, 3641. (c) See also: Nakamura, A.; Otsuka, S. *J. Am. Chem. Soc.* 1972, *94*, 1886; *J. Mol. Catal.* 1975/1976, *1*, 285.
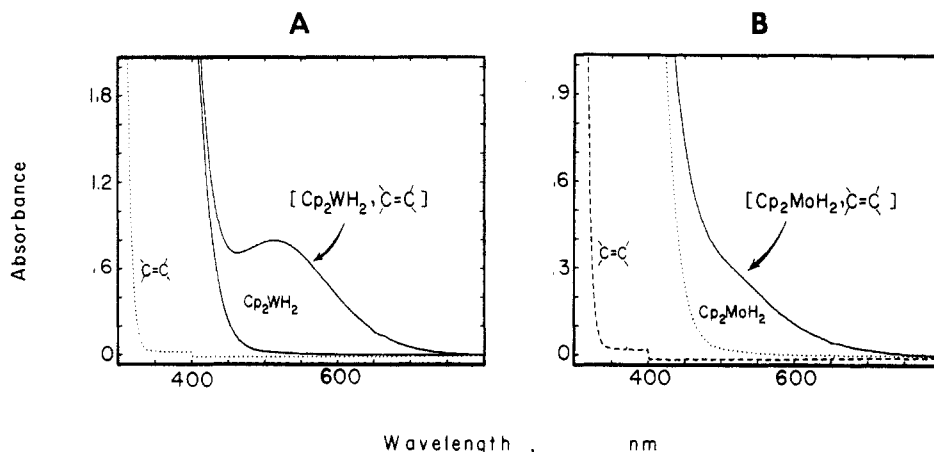
Figure 1. Charge-transfer absorption bands of the EDA complexes of (A) Cp_2WH_2 and (B) Cp_2MoH_2 with fumaronitrile in toluene in comparison with those of the uncomplexed donor and acceptor as indicated.
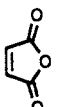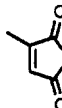
activation in eq 2 represents a useful rationale for the production of radical pairs.[16] The independent demonstration of such a mechanistic pathway would be provided by the photochemical promotion of hydrometalation from the EDA complex by the specific irradiation of the CT absorption band ($h\nu_{CT}$) under conditions in which the thermal process is too slow to compete.[17] Accordingly in this report we first elaborate on the CT spectra and formation constants of the EDA complexes of HM = Cp_2WH_2, Cp_2MoH_2, and Cp_2ReH with various electron acceptors as intermediates and then describe their direct involvement in the charge-transfer photochemistry leading to olefin hydrometalation and hydrogenation.

Results

Charge-Transfer Complexes of Cp_2MH_2 (M = Mo, W) and Cp_2ReH as Electron Donors with Olefinic Acceptors.

The pale yellow solution of Cp_2WH_2 in toluene immediately took on an intense red-orange coloration upon the addition of fumaronitrile. The spectral transformation accompanying this color change is shown in Figure 1A by the appearance of a new, broad absorption band with λ_{max} = 516 nm in comparison with the presence of only tail absorptions of Cp_2WH_2 and fumaronitrile with their low-energy cutoffs at ~450 and 330 nm, respectively. The homologue Cp_2MoH_2 produced an immediate orange coloration upon a similar treatment; the new absorption band shown in Figure 1B was blue-shifted to the extent sufficient to obscure its λ_{max} at ~450 nm.

Exposure of Cp_2WH_2 to the stronger acceptor maleic anhydride yielded a bright green solution with the new absorption band at λ_{max} = 538 nm. The spectral red shift from λ_{max} = 516 to 538 nm followed the increase in the electron affinity (EA) of the acceptor maleic anhydride (EA = 1.44 eV) relative to that of fumaronitrile (EA = 1.24 eV).[18] Moreover, the moderate acceptor citraconic anhydride with EA = 1.29 eV spontaneously produced a

Table I. Charge-Transfer Complexes of Hydridometal Donors with Activated Olefins[a]

olefin acceptor[b]	hydrido-metal donor	CT color[c]	$\epsilon,^d$ M^{-1} cm^{-1}	$K,^d$ M^{-1}
NC⌒⌒CN (1.24)	Cp_2WH_2	red-orange (516)	140	1.1
	Cp_2MoH_2	orange (~480)[e]	24[f]	7.3
	Cp_2ReH	red-orange (530)	140	0.77
(1.44)	Cp_2WH_2	green (538)	130	0.20
	Cp_2MoH_2	blue (530)	42	5.6
	Cp_2ReH	orange (g)	25[h]	7.1
(1.29)	Cp_2WH_2	violet (530)	130	0.3
	Cp_2MoH_2	orange (g)	190[f]	0.08
	Cp_2ReH	yellow-orange (~460)[e]	42[i]	1.2
MeO_2C⌒⌒CO_2Me	Cp_2WH_2	red-orange (480)[e]	260[h]	0.08
	Cp_2MoH_2	j		
	Cp_2ReH	yellow-orange (470)[e]	304[h]	0.07

[a] With 0.02 M Cp_2MH_2 and ~0.1 M acceptor in toluene at 25 °C. [b] Electron affinity (eV) in parentheses. [c] λ_{max} in parentheses (nm). [d] At λ_{max}, except as noted. [e] Shoulder. [f] At 520 nm. [g] Unresolved. [h] At 500 nm. [i] At 550 nm. [j] Thermal reaction too fast to measure.[13]

violet solution with Cp_2WH_2, in which the new absorption spectrum occurred at the intermediate value of λ_{max} = 530 nm.

According to Mulliken theory,[19] the direct relationship of the new absorption band to the electron affinity of the olefinic acceptor is associated with the charge-transfer excitation ($h\nu_{CT}$) of the EDA complex [HM,>C=C<]. Indeed, this spectral assignment is consistent with the blue shift of the new absorption band accompanying the change in donor from Cp_2WH_2 to Cp_2MoH_2 (as indicated in Table I for various acceptors) to accord with the corresponding diminution in the donor strength (vide infra).[20] The series of charge-transfer spectra of the related hydridometal donor Cp_2ReH with the same olefinic acceptors are also included in Table I for comparison.

The charge-transfer absorption bands arising from toluene and benzene solutions of Cp_2WH_2 and the olefinic acceptors were persistent at 25 °C in the dark, as judged

(14) Foster, R., Ed. *Molecular Complexes*; Elek Science: London, 1973; Vol. 1 and 2.

(15) For other examples of Cp_2MH_2 complexes, see: (a) Crotty, D. E.; Anderson, T. J.; Glick, M. D.; Oliver, J. P. *Inorg. Chem.* **1977**, *16*, 2346. (b) Storr, A.; Thomas, B. S. *Can. J. Chem.* **1971**, *49*, 2504. (c) Shriver, D. F. *J. Am. Chem. Soc.* **1963**, *85*, 3509. (d) Shriver, D. F.; Johnson, M. P. *J. Am. Chem. Soc.* **1966**, *88*, 301.

(16) Compare also: Hayes, J. C.; Cooper, N. J. *J. Am. Chem. Soc.* **1982**, *104*, 5570. Hayes, J. C.; Jernakoff, P.; Miller, G. A.; Cooper, N. J. *Pure Appl. Chem.* **1984**, *56*, 25.

(17) For a recent example see: (a) Klingler, R. J.; Mochida, K.; Kochi, J. K. *J. Am. Chem. Soc.* **1979**, *101*, 6626. (b) Wallis, J. M.; Kochi, J. K. *J. Am. Chem. Soc.* **1988**, *110*, 8207.

(18) (a) Paul, G.; Kebarle, P. *J. Am. Chem. Soc.* **1989**, *111*, 464. (b) Kebarle, P.; Chowdhury, S. *Chem. Rev.* **1987**, *87*, 513.

(19) Mulliken, R. S. *J. Am. Chem. Soc.* **1952**, *74*, 811. Mulliken, R. S.; Person, W. B. *Molecular Complexes*; Wiley: New York, 1969.

(20) See Table III.

A

B
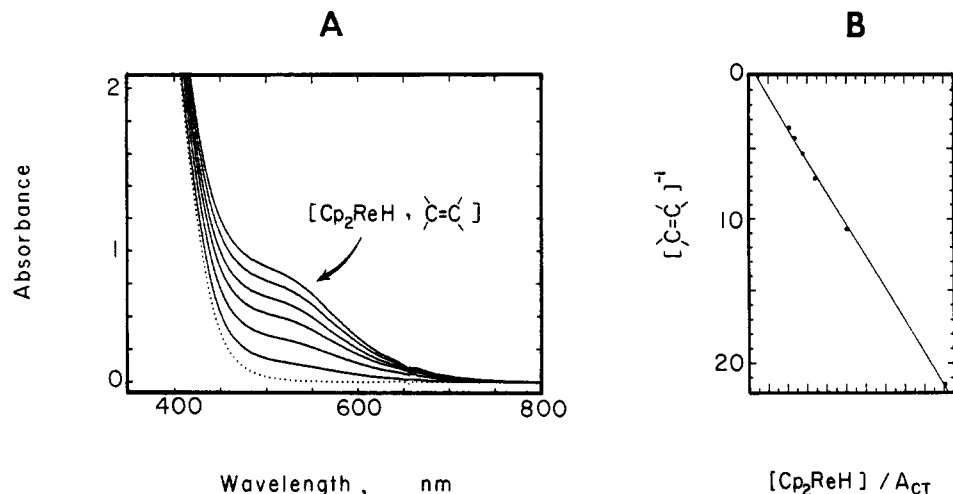
Figure 2. (A) Absorption spectra of 0.023 M Cp$_2$ReH with fumaronitrile (2-equiv increments; —) in toluene relative to that of Cp$_2$ReH alone (···). (B) Plot of the Benesi–Hildebrand relationship in eq 3 of the data in (A).

by the spectral invariance for >16 h. Similarly the CT spectra associated with the analogous donor Cp$_2$MoH$_2$ were unchanged for periods exceeding 10 h, but a slight (<5%) decrease in the CT absorbance was noted with fumaronitrile. However, the removal of solvent in vacuo resulted in the bleaching of the orange-red solution to yield a pale yellow solid, from which the unchanged Cp$_2$MoH$_2$ could be recovered quantitatively.[21] It follows that any thermal reaction possibly resulting from the donor–acceptor pairs included in Table I was too slow at 25 °C to provide any competition with the photochemical process examined (vide infra).

The formation constants of the EDA complexes in toluene solutions of Cp$_2$MoH$_2$, Cp$_2$WH$_2$, and Cp$_2$ReH with the olefinic acceptors were measured spectrophotometrically. According to the Benesi–Hildebrand method,[22] the concentration dependence of the absorbance of the charge-transfer band A_{CT} for the 1:1 EDA complex is given by

$$\frac{[Cp_2MH_2]}{A_{CT}} = \frac{1}{K\epsilon_{CT}}\frac{1}{[>C\!=\!C<]} + \frac{1}{\epsilon_{CT}} \quad (3)$$

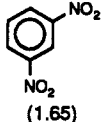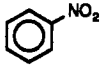under conditions in which the concentration of the electron acceptor [>C=C<] is in large excess relative to the concentration of the hydridometal donor [Cp$_2$MH$_2$].[23] Typically, Figure 2A illustrates the CT absorbance change accompanying the incremental addition of fumaronitrile to Cp$_2$ReH, and Figure 2B is the corresponding Benesi–Hildebrand plot evaluated at the monitoring wavelength of λ_{max}. The formation constant of $K = 0.77$ M^{-1} and the extinction coefficient of $\epsilon_{CT} = 143$ M^{-1} cm^{-1} of this EDA complex are listed in Table I (entry 1), together with those of the other hydridic donors (see columns 4 and 5).

$$Cp_2MH_2 + >C\!=\!C< \overset{K}{\rightleftharpoons} [Cp_2MH_2,>C\!=\!C<] \quad (4)$$
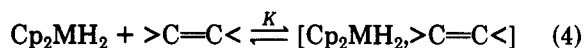
The limited magnitudes of the formation constants listed in Table I indicate that all the EDA complexes of the hydridometal donors with the olefinic acceptors are weak.[24] Although previous studies showed that single crystals of

Table II. Nitroarenes as Electron Acceptors with Cp$_2$MH Donors[a]

acceptor[b]	donor	CT color[c]	ϵ,[d] M^{-1} cm^{-1}	K,[d] M^{-1}
(1.65)	Cp$_2$WH$_2$	violet (568)	580	0.11
	Cp$_2$MoH$_2$	green[e]	62[f]	8.7
	Cp$_2$ReH	green[e]	1300[g]	0.06
(1.01)	Cp$_2$WH$_2$	red-orange (480)[i]	35[h]	0.06

[a] With 0.02 M Cp$_2$MH$_2$ and ~0.1 M nitroarene at 25 °C. [b] Electron affinity (eV) in parentheses. [c] λ_{max} in parentheses (nm). [d] At λ_{max} unless noted otherwise. [e] Unresolved. [f] At 500 nm. [g] At 550 nm. [h] At 494 nm. [i] Shoulder.

such weak EDA complexes could be obtained,[25] all attempts at the isolation of [Cp$_2$MH$_2$,>C=C<], including the freezing of various mixtures of the hydridometal in neat olefinic acceptors, merely led to phase separation and discharge of the CT color. Thus, the absorption bands illustrated in Figures 1–3 are properly ascribed to contact charge transfer[26] between the hydridometal donors and the olefinic acceptors. It is also noteworthy that solutions of Cp$_2$MH$_2$ and olefinic acceptors exhibited new CT absorption bands only in highly nonpolar solvents such as hydrocarbons and chloroalkanes.[27] In the more polar solvent acetonitrile, the intensity of the CT band was considerably attenuated and usually appeared unresolved as a shoulder on the tail absorption of the donor.

Nitroarenes as Electron Acceptors for Cp$_2$MH$_2$ Donors. Nitroarenes by virtue of their relatively high electron affinities are representative of highly delocalized electron π-acceptors.[28] Similar to the olefinic acceptors, nitrobenzene and dinitrobenzene afforded orange and violet solutions, respectively, when added to Cp$_2$WH$_2$ dissolved in toluene.[13] Moreover, the typical red shift of the CT spectrum accompanying the change from nitrobenzene to the stronger acceptor is shown in Figure 3. Comparison of the CT data and the formation constants

(21) Compare with the behavior of the contact charge-transfer complex of OsO$_4$ and arenes in ref 17b. See also: (a) Hammond, P. R.; Lake, R. R. *J. Chem. Soc. A* **1971**, 3819. (b) Burkardt, L. A.; Hammond, P. R.; Knipe, R. H.; Lake, R. R. *J. Chem. Soc. A* **1971**, 3789.

(22) Benesi, H. A.; Hildebrand, J. H. *J. Am. Chem. Soc.* **1949**, 71, 2703.

(23) Person, W. B. *J. Am. Chem. Soc.* **1965**, 87, 167.

(24) Foster, R., Ed. *Molecular Association*; Academic: New York, 1975; Vol. 1.

(25) See for example: Takahashi, Y.; Sankararaman, S.; Kochi, J. K. *J. Am. Chem. Soc.* **1989**, 111, 2954. Blackstock, S. C.; Kochi, J. K. *J. Am. Chem. Soc.* **1987**, 109, 2484; *J. Org. Chem.* **1987**, 52, 1451.

(26) Tamres, M.; Strong, R. L. In ref 24, Vol. 2, p 340ff (1979).

(27) Compare: Wallis, J. M.; Kochi, J. K. In ref 17b.

(28) (a) Chowdhury, S.; Heinis, T.; Grimsrud, E. P.; Kebarle, P. *J. Phys. Chem.* **1986**, 90, 2747. (b) Chowdhury, S.; Heinis, T.; Kebarle, P. *J. Am. Chem. Soc.* **1986**, 108, 4662.
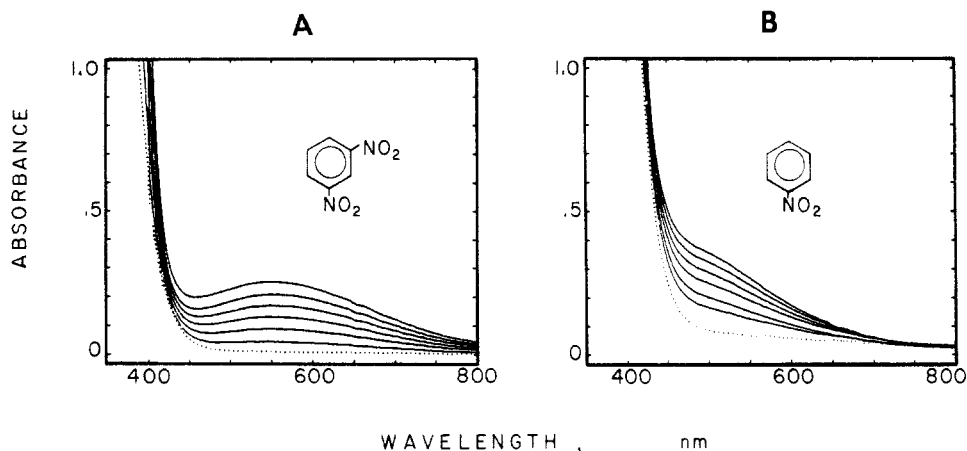
Figure 3. Bathochromic shift of the charge-transfer absorption band of the EDA complex of 0.044 M Cp₂WH₂ with *m*-dinitrobenzene (A) relative to that of nitrobenzene (B), both with successive 3-equiv increments in toluene solution.

in Table II for the nitroarene acceptors with those of the corresponding olefinic acceptors in Table I indicates that similar delocalized structures were pertinent to both series of EDA complexes. Furthermore, these are, with minor discrepancies, equivalent to those reported earlier by Nakamura and Otsuka.[13b]

Charge-Transfer Photochemistry of Cp₂MoH₂ and Fumaronitrile. Although the deep orange solution of Cp₂MoH₂ and 5 equiv of fumaronitrile remained unchanged at 25 °C for prolonged periods, the color was rapidly discharged (<3 h) when the toluene solution was deliberately exposed to the filtered actinic output with λ > 550 nm from a 500-W mercury lamp. The bleaching of the CT color was accompanied by the separation (95% yield) of a yellow-orange precipitate that obviated a meaningful measurement of the quantum yield for the charge-transfer photochemistry. Since Cp₂MoH₂ is known to eliminate dihydrogen upon UV irradiation,[29] a control experiment was also carried out under the same conditions, but without added fumaronitrile. The UV spectrum of Cp₂MoH₂ in toluene was unchanged after 64 h of irradiation. Indeed, inspection of Figure 1B shows that Cp₂MoH₂ is transparent to actinic radiation with λ > 550 nm, and it could therefore only excite the charge-transfer band of the EDA complex. Thus, in these studies there could be no ambiguity about either the adventitious local excitation of the uncomplexed donor (acceptor) or the generation of intermediates other than those arising directly from the charge-transfer excitation of [Cp₂MH₂, >C=C<].

The elemental analysis of the yellow-orange precipitate was consistent with its formulation as the 1:1 adduct I, i.e.

$$Cp_2MoH_2 + NCCH=CHCN \xrightarrow{h\nu_{CT}}$$
$$\underset{I}{Cp_2Mo(CHCNCH_2CN)H} \quad (5)$$
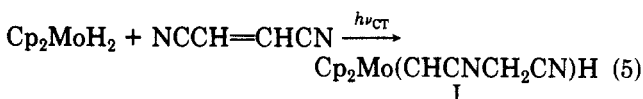
This structural assignment of I was supported by its ¹H NMR spectrum, showing a single hydridic resonance at δ −8.56 and an ABX splitting pattern for the alkyl protons (δ 1.91, 2.40, 2.49), and the ¹³C NMR spectrum, showing the pair of alkyl carbon centers at δ −12.85 (coordinated to Mo) and 26.04.[30] Although the ¹³C NMR spectrum revealed the diastereotopic Cp ligands at δ 85.6 and 85.5, the ¹H NMR spectrum showed only an unresolved singlet

Figure 4. ORTEP diagram of the hydrido alkyl σ-adduct I from the charge-transfer photochemistry of Cp₂MoH₂ and fumaronitrile.
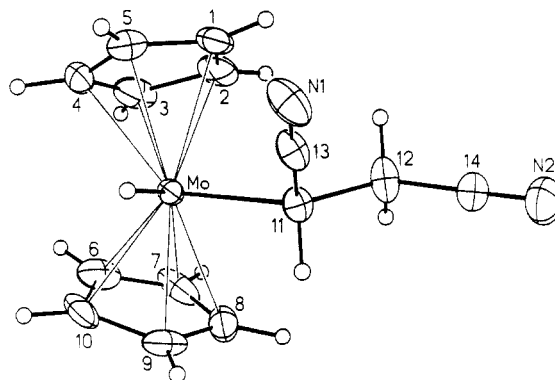
resonance at δ 5.02. Unfortunately, alkylmolybdenum hydrides of this type are unknown for help in the resolution of this ambiguity. Since the identity of I was critical for the establishment of charge-transfer hydrometalation, we deemed it necessary to grow a single crystal of the yellow-orange precipitate for an unequivocal structure elucidation by X-ray crystallography (see Experimental Section).

X-ray Crystallography of the Charge-Transfer Adduct I from Cp₂MoH₂ and Fumaronitrile. The structure of I was solved in the monoclinic space group *P*2₁ by using Patterson techniques to locate the Mo atom and by using successive least-squares and difference Fourier calculations to obtain the positions of the other (non-hydrogen) atoms. The hydrido ligand attached to Mo was located in a difference map. Since the yellow-orange adduct crystallized in a chiral space group, the Rogers test[31] was performed to obtain the correct absolute configuration shown by the ORTEP diagram in Figure 4. The latter thus established the CT photochemistry of the EDA complex [Cp₂MoH₂,>C=C<] to afford the σ-adduct I, which is structurally akin to others obtained by thermal hydrometalations.[13a] Thus, the Mo–C distance of 2.22 Å in I is comparable to that for hydrocarbyl derivatives found in various cyclopentadienylmolybdenum complexes, including Cp₂Mo(C₂H₅)Cl (2.28 Å),[32] Cp₂Mo(NO)(C₅H₅) (2.29 Å),[33] CpMo(CO)₃C₃F₇ (2.29 Å),[34] and Cp₂Mo[C(CO₂Me)-

(29) Geoffroy, G. L.; Bradley, M. G. *J. Organomet. Chem.* **1977,** *134,* C27.

(30) The adduct I was previously isolated[13a] but was incompletely characterized.

(31) Rogers, D. *Acta Crystallogr.* **1981,** *A37,* 734.

(32) Prout, K.; Cameron, T. S.; Forder, R. A.; Critchley, S. R.; Denton, B.; Rees, G. V. *Acta Crystallogr.* **1974,** *B30,* 2290.

(33) Calderon, J. L.; Cotton, F. A.; Legzdins, P. *J. Am. Chem. Soc.* **1969,** *91,* 2528.

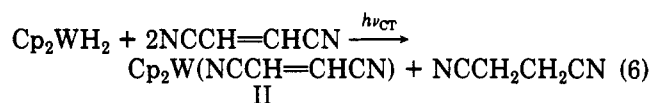(34) Churchill, M. R.; Fennessey, J. P. *Inorg. Chem.* **1967,** *6,* 1213.

=CHCO$_2$Me]H (2.22 Å).[6e,35] The η^5-Cp$_2$Mo fragment in I is comparable to those generally extant in the bent d^2 metallocene complexes, insofar as the mean Mo distance to the Cp centroid of 1.99 Å and Cp–Mo–Cp dihedral angle of 120° are concerned.[36]

Charge-Transfer Photochemistry of Cp$_2$WH$_2$ and Fumaronitrile. Owing to the similarity of Cp$_2$WH$_2$ and Cp$_2$MoH$_2$ in their photoinduced elimination of dihydrogen by UV (366 nm) light,[29,37] we examined the charge-transfer photochemistry of Cp$_2$WH$_2$ and fumaronitrile under conditions identical with those employed for Cp$_2$MoH$_2$ in eq 5. Thus, the use of the same filtered actinic output with λ > 550 nm ensured the photoexcitation of only the charge-transfer band of the EDA complex [Cp$_2$WH$_2$,>-C=C<] and not the local band[38] of the hydridometal donor, as established by the comparison of the absorption spectra in Figure 1A.
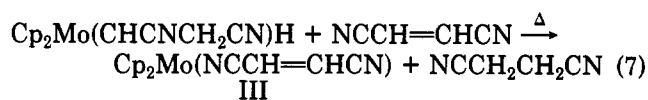
The orange-red solution of Cp$_2$WH$_2$ containing 5 equiv of fumaronitrile in toluene was unchanged even when heated at 100 °C for 6 h. However, its exposure to the filtered radiation with λ > 550 nm at 25 °C (vide supra) caused a gradual bleaching of the CT color, accompanied by the slow separation of a red-brown crystal, much like that observed with Cp$_2$MoH$_2$ (vide supra). Although such a simultaneous precipitation precluded quantitative measurements, the significantly longer radiation times of 60 h required for the CT process with Cp$_2$WH$_2$ to attain 40% conversion indicated a qualitatively (factor of ~50) lower photoefficiency compared to that in eq 5 for Cp$_2$MoH$_2$. Spectral (IR, ^{1}H and ^{13}C NMR) analysis of the red-brown crystals II revealed a 3:2 molar mixture of fumaronitrile and maleonitrile π-complexed to tungstenocene (see the Experimental Section for details). Along with the observation of succinonitrile (95%), the stoichiometry of the CT photochemistry of the hydridotungsten complex was readily described as

$$\text{Cp}_2\text{WH}_2 + 2\text{NCCH}{=}\text{CHCN} \xrightarrow{h\nu_{CT}}$$
$$\text{Cp}_2\text{W(NCCH}{=}\text{CHCN)} + \text{NCCH}_2\text{CH}_2\text{CN} \quad (6)$$
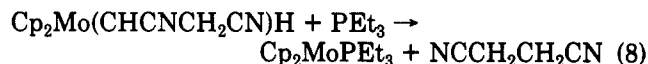$$\text{II}$$

Thermal and Photochemical Transformation of the Hydridoalkylmolybdenum Adduct I. The different stoichiometries for the charge-transfer photochemistry of Cp$_2$MoH$_2$ and Cp$_2$WH$_2$ complexes with fumaronitrile in eqs 5 and 6, respectively, could have arisen from a further reductive elimination of the putative hydridoalkyltungsten adduct allowed by the longer times for this photoreaction. In order to examine this possibility, the course of the corresponding σ-adduct I was examined under both thermal and photochemical conditions somewhat similar to those extant during charge-transfer activation.

The *thermal decomposition* of the hydridoalkyl adduct I was carried out in dimethyl sulfoxide owing to its insolubility in hydrocarbon solvents. Typically in this solvent, a 4 mM solution of I with 5 equiv of added fumaronitrile was completely decomposed within 90 min at 95 °C. Chromatographic analysis of succinonitrile and spectral (^{1}H NMR) analysis of a 3:2 mixture of fumaronitrile and maleonitrile π-adducts III to molybdenocene

indicated the stoichiometry for the thermal decomposition to be

$$\text{Cp}_2\text{Mo(CHCNCH}_2\text{CN)H} + \text{NCCH}{=}\text{CHCN} \xrightarrow{\Delta}$$
$$\text{Cp}_2\text{Mo(NCCH}{=}\text{CHCN)} + \text{NCCH}_2\text{CH}_2\text{CN} \quad (7)$$
$$\text{III}$$

An analogous reductive elimination of I carried out with added triethylphosphine was complete in 15 min at 95 °C to yield succinonitrile and molybdenocene as the phosphine adduct[38] in quantitative yields, i.e.

$$\text{Cp}_2\text{Mo(CHCNCH}_2\text{CN)H} + \text{PEt}_3 \rightarrow$$
$$\text{Cp}_2\text{MoPEt}_3 + \text{NCCH}_2\text{CH}_2\text{CN} \quad (8)$$

Furthermore, the hydrido alkyl adduct I was completely decomposed by carbon tetrachloride at room temperature within 30 min by chlorinolysis of the Mo–H bond to afford chloroform, i.e.[39]

$$\text{Cp}_2\text{Mo(CHCNCH}_2\text{CN)H} + \text{CCl}_4 \rightarrow$$
$$\text{Cp}_2\text{Mo(CHCNCH}_2\text{CN)Cl} + \text{HCCl}_3 \quad (9)$$

The *photochemical transformation* of the hydrido alkyl σ-adduct I was also carried out (under the same conditions as in eq 7) by irradiating the solution with the filtered actinic output with λ > 550 nm (vide supra) at 25 °C. Analysis of the photolysate after 24 h indicated a 28% conversion of I to the same 3:2 mixture of the fumaronitrile–maleonitrile adducts III of molybdenocene described in eq 7, together with an equivalent amount of succinonitrile, i.e.

$$\text{Cp}_2\text{Mo(CHCNCH}_2\text{CN)H} + \text{NCCH}{=}\text{CHCN} \xrightarrow[{>550 \text{ nm}}]{h\nu}$$
$$\text{Cp}_2\text{Mo(NCCH}{=}\text{CHCN)} + \text{NCCH}_2\text{CH}_2\text{CN} \quad (10)$$
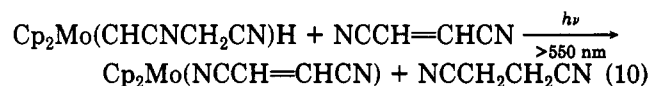
Moreover, the control experiment confirmed the absence of competition (<3%) from the thermal process (eq 7) at these reduced temperatures.

Maleic Anhydride as an Olefinic Acceptor for Cp$_2$MH$_2$. The exposure of the green solution of Cp$_2$WH$_2$ and maleic anhydride in toluene at 25 °C to the filtered light with λ > 550 nm (vide supra) resulted in the excitation of only the low-energy tail of the CT absorption band (see Table I). The gradual discharge of charge-transfer color was accompanied by the separation from solution of red-brown crystals of the maleic anhydride π-adduct IV of tungstenocene (see Experimental Section). This coupled with the presence of an equimolar amount of succinic anhydride in solution indicated the stoichiometry of the charge-transfer photochemistry to be cleanly described as

 (11)
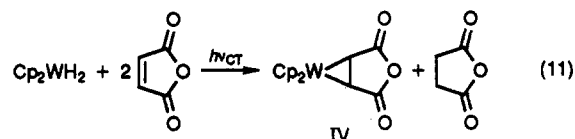
The charge-transfer excitation of the blue solution of the EDA complex of Cp$_2$MoH$_2$ and maleic anhydride occurred in much the same manner as that described in eq 11 to afford the analogous π-adduct V of molybdenocene and succinic anhydride, albeit with higher photoefficiency (see Experimental Section). Indeed, the π-adducts IV and V from Cp$_2$WH$_2$ and Cp$_2$MoH$_2$ both consisted of a single isomer, each with differentiated Cp ligands in the ^{1}H and ^{13}C NMR spectra arising from the magnetic anisotropy of the cyclic anhydride functionality. No evidence of the

(35) The Mo–H bond of 1.53 Å is slightly shorter than that (1.69 Å) found in the precursor Cp$_2$MoH$_2$. See: Schultz, A. J.; Stearley, K. L.; Williams, J. M.; Mink, R.; Stucky, G. D. *Inorg. Chem.* **1977**, *16*, 3303.

(36) (a) Churchill, M. R.; Fennessey, J. P. In ref 34. (b) Wolczanski, P. T.; Threlkel, R. S.; Santarsiero, B. D. *Acta Crystallogr.* **1983**, *C39*, 1330.

(37) (a) Giannotti, C.; Green, M. L. H. *J. Chem. Soc., Chem. Commun.* **1972**, 1114. (b) Farrugia, L.; Green, M. L. H. *J. Chem. Soc., Chem. Commun.* **1975**, 416. (c) Berry, M.; Elmitt, K.; Green, M. L. H. *J. Chem. Soc., Dalton Trans.* **1979**, 1950.

(38) Geoffroy, G. L.; Bradley, M. G. *Inorg. Chem.* **1978**, *17*, 2410.

(39) See: Kochi, J. K. *Organometallic Mechanisms and Catalysis*; Academic: New York, 1978; pp 506–509.
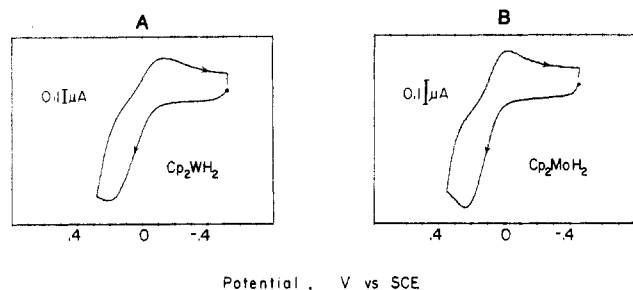
Figure 5. Fast-scan cyclic voltammetry with a platinum microelectrode (ϕ = 5 μm) in acetonitrile containing 0.1 M tetra-*n*-butylammonium hexafluorophosphate of (A) 0.01 M Cp$_2$WH$_2$ at 8 kV s^{-1} and (B) 0.01 M Cp$_2$MoH$_2$ at 5 kV s^{-1}.

Table III. Fast-Scan Cyclic Voltammetry of Hydridometal Donors[a]

scan rate, kV s⁻¹	Cp₂WH₂			Cp₂MoH₂		
	$E_p{}^a$	$E_p{}^c$	$E°_{ox}$	$E_p{}^a$	$E_p{}^c$	$E°_{ox}$
0.5	0.12	b		0.23	b	
1.0	0.18	b		0.27	b	
2.0	0.16	-0.16	0	0.29	b	
5.0	0.17	-0.15	0.01	0.24	0.02	0.13
8.0	0.21	-0.15	0.03			
10.0	0.18	-0.13	0.02	0.33	-0.08	0.14
20.0	0.19	-0.18	0	0.30	-0.05	0.13

[a] With 0.01 M Cp$_2$MH$_2$ in acetonitrile containing 0.1 M tetra-*n*-butylammonium hexafluorophosphate; in V vs SCE at 25 °C. $E_p{}^a$ = anodic peak potential on initial positive scan. $E_p{}^c$ = cathodic peak potential on return scan. $E°_{ox} = (E_p{}^a + E_p{}^c)/2$. [b] Cathodic peak not observed.

hydridoalkyl σ-adduct (related to I derived from fumaronitrile) was found. Furthermore, the control experiments established that there was no thermal process to compete with the photoreduction of maleic anhydride with either Cp$_2$MoH$_2$ or Cp$_2$WH$_2$.

Oxidation Potentials of Cp$_2$MH$_2$ (M = W, Mo). Owing to the facile participation of the hydridometal donors Cp$_2$WH$_2$ and Cp$_2$MoH$_2$ in the charge-transfer photochemistry described above, it was important to establish the driving force for their one-electron oxidation. The previous electrochemical study indicated that the initial positive-scan cyclic voltammetry (CV) of Cp$_2$WH$_2$ was irreversible at conventional sweep rates due to the transient character of the 17-electron cation radical Cp$_2$WH$_2$·+ in acetonitrile.[40] Since faster CV scan rates can be achieved with the newly developed ultramicroelectrodes,[41] the reversible oxidation of Cp$_2$WH$_2$ and Cp$_2$MoH$_2$ was reinvestigated. Typically, platinum microelectrodes (ϕ = 5 μm) were used at sweep rates up to 20 000 V s^{-1} in acetonitrile solutions of Cp$_2$WH$_2$ containing 0.1 M tetra-*n*-butylammonium hexafluorophosphate as the supporting electrolyte. Figure 5A clearly shows the presence of the well-defined cathodic wave $E_p{}^c$ following the appearance of the anodic wave at $E_p{}^a$ = 0.17 V vs SCE when the cyclic voltammetry of Cp$_2$WH$_2$ was carried out at 5000 V s^{-1}. The validity of the measured reversible oxidation potential $E°_{ox}$ is shown by the constancy of $(E_p{}^c + E_p{}^a)/2$ in columns 4 and 7 of Table III:

$$Cp_2MH_2 \underset{}{\overset{E°_{ox}}{\rightleftharpoons}} Cp_2MH_2\text{·+} + e^- \qquad (12)$$

(Note that when both the anodic and cathodic CV waves

(40) Klingler, R. J.; Huffman, J. C.; Kochi, J. K. *J. Am. Chem. Soc.* **1980**, *102*, 208.

(41) Howell, J. O.; Wightman, R. M. *Anal. Chem.* **1984**, *56*, 524. Wipf, D. O.; Kristensen, E. W.; Deakin, M. R.; Wightman, R. M. *Anal. Chem.* **1988**, *60*, 306.

Electron Affinity, eV

Figure 6. Mulliken plot of the charge-transfer excitation energies ($h\nu_{CT}$) of the EDA complexes of various acceptors (as indicated) with Cp$_2$MoH$_2$ ($\ominus$), Cp$_2$WH$_2$ ($\bullet$) and Cp$_2$ReH (O).

are visible as in Figure 5, the standard oxidation potential $E°_{ox}$ must lie within the interval $(E_p{}^c + 30$ mV) $< E°_{ox} < (E_p{}^a - 30$ mV)).[42]

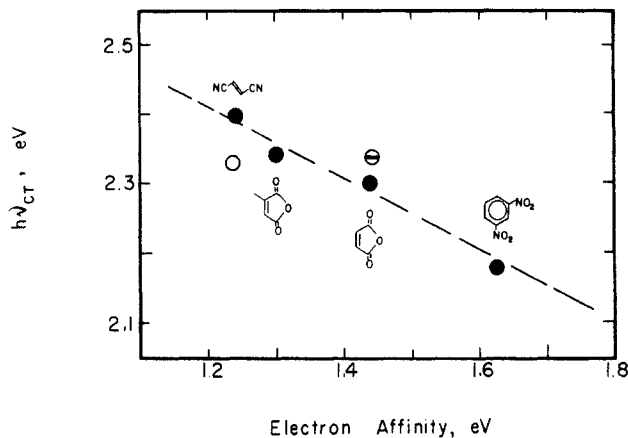Inspection of Figure 5B shows that the one-electron oxidation of Cp$_2$MoH$_2$ was also reversible at CV rates exceeding 5000 V s^{-1}. The accurate determination of $E°_{ox}$ allowed in this manner indicated that the driving force for the oxidation of Cp$_2$WH$_2$ was more favorable than that of Cp$_2$MoH$_2$ by 0.13 V or 3 kcal mol^{-1}. Such a slight difference in the energetics of electron detachment also pertained to the gas-phase processes, since the ionization potentials of both have been reported to be 6.4 eV, within the resolution of the photoelectron spectrometer.[43]

Discussion

The tungsten and molybdenum hydrides Cp$_2$WH$_2$ and Cp$_2$MoH$_2$ are electron-rich by virtue of their low ionization potentials in the gas phase[43] and reversible oxidation potentials in solution (Table III). As such, the striking colors that are developed in the presence of activated olefins (Table I) are typical of electron donor–acceptor complexes with charge-transfer absorptions.[44] The limited magnitudes of the formation constants K in eq 4 indicate that the intermolecular interactions within the 1:1 complexes [Cp$_2$MH$_2$,>C=C<] are weak. Importantly, the linear correlation of the charge-transfer transition energy ($h\nu_{CT}$) with the electron affinity of activated olefins in Table I is a direct consequence of Mulliken theory.[19] The general applicability of the latter is shown by the inclusion in Figure 6 of the structurally distinct nitroarene among the olefinic acceptors in their common charge-transfer interactions[44] with the hydridometal donors. Although we have as yet been unable to grow a single crystal of an EDA complex for the X-ray crystallographic determination of the acceptor–donor structure, it is reasonable to expect the olefin to lie proximally to a plane between the bent-back Cp rings (Figure 4) of the hydridometal. If so, the LUMO of the olefinic acceptor can overlap with the HOMO consisting of the a_1 ligand orbital of the Cp$_2$MH$_2$ donor[45] to describe a nonbonded π^*-σ interaction in the EDA complex. Be that as it may, electron transfer within the HOMO–LUMO gap is spontaneously induced by the direct

(42) Nicholson, R. S. *Anal. Chem.* **1965**, *37*, 1351.

(43) Green, J. C.; Jackson, S. E.; Higginson, B. *J. Chem. Soc., Dalton Trans.* **1975**, 403.

(44) See: Foster, R. *Organic Charge-Transfer Complexes*; Academic: New York, 1969.

(45) Lauher, J. W.; Hoffmann, R. *J. Am. Chem. Soc.* **1976**, *98*, 1729. See also: Albright, T. A.; Burdett, J. K.; Whangbo, M. H. *Orbital Interactions in Chemistry*; Wiley: New York, 1985.

irradiation of the charge-transfer absorption band of such weak EDA complexes.[46]   The resultant photoinduced charge separation leads to the ion radical pair in eq 13.

$$[Cp_2MH_2,>C=C<] \xrightarrow{h\nu_{CT}} [Cp_2MH_2^{\bullet+}, >C^-\!\!-\!\!C^\bullet <]$$
$$\text{EDA complex} \qquad\qquad \text{ion radical pair}$$

(13)

This formulation is based on Mulliken's theory of charge transfer, and it derives experimental verification from our direct observation of various transient ion radical pairs by time-resolved spectroscopic studies on the picosecond time scale.[47]

Charge-Transfer Photochemistry Leading to Olefin Hydrometalation. The seminal role of the CT ion pair $[Cp_2MH_2^{\bullet+},>C^-\!\!-\!\!C^\bullet<]$ as the obligatory intermediate from the photoexcitation of the EDA complex must be included in any mechanistic formulation of olefin hydrometalation by taking particular cognizance of how it decays. Especially relevant to the issue here is the fate of the donor moiety $Cp_2MH_2^{\bullet+}$ in the ion radical pair. Indeed the previous electrochemical generation of $Cp_2WH_2^{\bullet+}$ in acetonitrile established its transient existence arising from the facile proton loss in eq 14.[40]

$$Cp_2MH_2^{\bullet+} \xrightarrow[\text{MeCN}]{} Cp_2MH^\bullet + H_{MeCN}^+ \qquad (14)$$

Such a proton transfer when it occurs within the CT ion radical pair (eq 13) will result in the corresponding radical pair, i.e.

$$\left[Cp_2MH_2^{\bullet+}, >\!\!\overset{\bullet}{C}\!\!-\!\!\overset{\bullet}{C}\!\!< \right] \longrightarrow \left[Cp_2MH^\bullet, -\!\!\overset{H}{\underset{|}{C}}\!\!-\!\!\overset{\bullet}{C}\!\!< \right] \qquad (15)$$

The homolytic coupling of the radical pair constitutes a mechanistic basis of CIDNP,[10] and it is expected to occur with little if any activation energy.[48] Accordingly, the most direct path to the charge-transfer photochemistry of Cp_2MH_2 leading to olefin hydrometalation includes two discrete steps in eq 18 and 19 following the pre-equilibrium formation and charge-transfer excitation of the EDA complex, viz.[49] Scheme II. Thus, the formation of the hydridoalkyl adduct I in high yields from the molybdenum hydride Cp_2MoH_2 in eq 5 will proceed via a multistep pathway involving at least four types of organic and organometallic radicals. Importantly, such a stepwise assemblage of reactive intermediates with high efficiency has been previously shown to occur during olefin hydrometalation with the hydridometal derivatives of the main-group elements tin, germanium, and silicon.[17a] In a more general context, quantitative photochemistry and time-resolved spectroscopy have established how the regiospecific sequence of ion-pair and radical-pair annihilations[51,52] can follow from the charge separation attendant upon the CT excitation of EDA complexes.[53]

Charge-Transfer Photochemistry Leading to Olefin Hydrogenation. The different course taken in eq 6 for the charge-transfer photochemistry of the tungsten hydride is hereafter referred to as olefin hydrogenation. Such an overall transformation of Cp_2WH_2 may involve a prior

Scheme II

Scheme III

hydrometalation of the olefin. Thus, the reductive elimination from the hydridoalkyltungsten adduct in a subsequent step, followed by the facile olefination of the reduced metallocene[54] (i.e. Scheme III) would account for the succinonitrile and the π-adduct II of tungstenocene in eq 6. Indeed, the isolation and separate decomposition of the isolable hydridoalkylmolybdenum adduct I in the presence of olefin indicate the viability of such a process (viz., eq 10) under the photochemical conditions extant during the charge-transfer photochemistry. The different stoichiometries obtained in eqs 5 and 6 for Cp_2MoH_2 and Cp_2WH_2, respectively, could then be accounted for by either (a) the rapid removal of I from solution owing to its insolubility or (b) the susceptibility of the putative hydridoalkyltungsten adduct to reductive elimination. We hasten to add that the product differentiation represented by eqs 5 and 6 is not necessarily unique to the molybdenum (versus tungsten) center in the donor, since Cp_2WH_2 and Cp_2MoH_2 both lead to olefin hydrogenation together with the π-adducts IV and V in the course of their charge-transfer photochemistry with maleic anhydride.

Olefin hydrogenation could alternatively arise directly from the radical pair in Scheme II (eq 18) by its disproportionation; i.e.

$$\left[Cp_2MH^\bullet, -\!\!\overset{H}{\underset{|}{C}}\!\!-\!\!\overset{\bullet}{C}\!\!< \right] \longrightarrow \left[Cp_2M, -\!\!\overset{H}{\underset{|}{C}}\!\!-\!\!\overset{H}{\underset{|}{C}}\!\!- \right], \text{etc.} \qquad (22)$$

as deduced from other CIDNP results.[10] Since radical coupling (eq 19) and radical disproportionation (eq 22) are likely to be competitive,[55] this possibility offers a unified view of hydrometalation and hydrogenation. Unfortunately we have not yet found a system that either exhibited photo-CIDNP or generated photostable σ-adducts to allow a further mechanistic delineation. Nonetheless, it is clear

(46) (a) Nagakura, S. In *Excited States*; Lim, E. C., Ed.; Academic: New York, 1975; Vol. 2. (b) Mataga, N. *Pure Appl. Chem.* **1984**, *56*, 1255. (c) Jones, G., II In *Photoinduced Electron Transfer*; Fox, M. A., Chanon, M., Eds.; Elsevier: Amsterdam, 1988; Part C, p 245ff.

(47) (a) Hilinski, E. F.; Masnovi, J. M.; Kochi, J. K.; Rentzepis, P. M. *J. Am. Chem. Soc.* **1984**, *106*, 8071. (b) Wallis, J. M.; Kochi, J. K. In ref 17b. See also: Takahashi, Y.; et al. In ref 25.

(48) Compare: Ingold, K. U. In *Free Radicals*; Kochi, J. K., Ed.; Wiley: New York, 1973, Vol. 1, p 38ff.

(49) The importance of back electron transfer[50] in eq 17 cannot be assessed at this juncture owing to the lack of quantum yield data.

(50) Fox, M. A. *Adv. Photochem.* **1986**, *13*, 237.

(51) Masnovi, J. M.; Kochi, J. K. *J. Am. Chem. Soc.* **1985**, *107*, 7880; *J. Org. Chem.* **1985**, *50*, 5245.

(52) The rate of radical coupling in eq 19 will determine the degree of stereospecificity in hydrometalation.

(53) Masnovi, J. M.; Kochi, J. K.; Hilinski, E. F.; Rentzepis, P. M. *J. Am. Chem. Soc.* **1986**, *108*, 1126.

(54) See: Thomas, J. L. *J. Am. Chem. Soc.* **1973**, *95*, 1838. See also ref 37 and 38. Note that the ground states of molydenocene and tungstenocene are paramagnetic, as shown by matrix isolation studies. See: Cox, P. A.; Grebenik, P.; Perutz, R. N.; Robinson, M. D.; Grinter, R.; Stern, D. R. *Inorg. Chem.* **1983**, *22*, 3614.

(55) For example, see: Benson, S. W. *Adv. Photochem.* **1964**, *2*, 1. See also ref 48.

that the metallocene precursors to the π-adducts II, III, and IV obtained in olefin hydrogenation are produced during charge-transfer photochemistry by a pathway which is distinctly different from Cp$_2$M previously produced by the direct irradiation of the hydridometal Cp$_2$MH$_2$, e.g.[37,38]

$$Cp_2MoH_2 \xrightarrow[366 \text{ nm}]{h\nu} Cp_2Mo + H_2 \qquad (23)$$
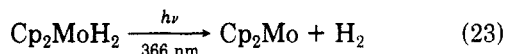
The photoinduced reductive elimination of molecular hydrogen in eq 23 is a relatively high-energy process, arising as it does from the population of the antibonding orbital of Cp$_2$MH$_2$ upon ultraviolet (as opposed to visible) irradiation.[56]

It is important to emphasize that Cp$_2$MoH$_2$ shows generally enhanced reactivity relative to that of Cp$_2$WH$_2$ in charge-transfer photochemistry, irrespective of whether olefin hydrometalation or hydrogenation pertains. Since the activation process involving charge separation in eq 15 is common to both processes, the kinetics differentiation must lie in the relative rates of proton transfer from the hydridometal cation radical in the follow-up step (eq 18). Indeed, the small difference in the thermodynamic stabilities of such metastable cation radicals as Cp$_2$MoH$_2^{\bullet+}$ and Cp$_2$WH$_2^{\bullet+}$ ($\Delta G \cong 3$ kcal/mol in Table III)[57] can easily translate into a factor of an order of magnitude in their kinetic acidities, especially toward such weak bases as the acceptor anion radicals in eq 18.[58]

Comments on the Thermal Hydrometalation of Olefins.

The pattern of charge-transfer photochemistry leading to olefin hydrometalation and hydrogenation by Cp$_2$MoH$_2$ and Cp$_2$WH$_2$ examined in this study bears a striking relationship to those previously effected thermally.[13] In general, the actinic input allows the charge-transfer activation to occur under conditions in which the thermal process is too slow to observe at ambient temperatures, and thus a direct, quantitative comparison of the two is difficult to make. However, the thermal hydrometalation of fumarate and maleate esters with Cp$_2$MoH$_2$ followed by the separate conversion of the σ-adduct to succinate esters[13a] has its counterpart in the CT photochemistry of the same acceptor–donor pairs leading directly to olefin hydrogenation.[60] In this system, the competition from the fast thermal hydrometalation unfortunately precludes its unambiguous observation by charge-transfer activation. Nonetheless the formation of the related hydridoalkyl adduct I from Cp$_2$MoH$_2$ and fumaronitrile via charge-transfer photochemistry corresponds to the analogous hydridoalkyl adduct[13a] from Cp$_2$MoH$_2$ and fumarate esters.

Since the reactivity of Cp$_2$MoH$_2$ in thermal hydrometalations shows the same strong dependence on the electron affinity of the activated olefin[13] as that observed in charge-transfer photochemistry (vide infra), similar activation barriers may be involved. Such a formulation is presented in eq 2 (Scheme I) as an electron transfer from Cp$_2$MH$_2$—analogous to that effected electrochemically at an anode (see eq 12). Thermal activation by electron transfer is akin to charge-transfer activation (eq 17) in the photoinduced process insofar as it generates an adiabatic ion pair that primarily differs from the vertical ion pair

by solvation.[61] Since proton transfer from the donor moiety (i.e., Cp$_2$MH$_2^{\bullet+}$) is facile (see eq 14), the kinetics distinction between these ion pairs is expected to be minimal.[62] We hope that a further search for (HM)/(olefin) pairs, in which the thermal and CT photochemical processes are competitive, will provide the opportunity to examine this relevant question further.

Experimental Section

Materials. Cp$_2$WH$_2$ and Cp$_2$MoH$_2$ were prepared according to published procedures.[63] Fumaronitrile and citraconic anhydride (Aldrich) were used as received. Maleic anhydride (Aldrich) was sublimed before use. m-Dinitrobenzene (Aldrich) was recrystallized from ethanol, and nitrobenzene (Du Pont) was distilled under reduced pressure. Toluene and benzene (Mallinckrodt) were stirred with concentrated sulfuric acid overnight, washed with dilute, aqueous NaOH, and distilled from sodium benzophenone. Acetonitrile (Mallinckrodt) was stirred over KMnO$_4$ for 24 h; the mixture was filtered and then distilled. The distillate was refluxed over phosphorus pentoxide; the mixture was filtered and then redistilled under an argon atmosphere from calcium hydride. Tetrahydrofuran (Du Pont) was distilled from sodium benzophenone. All the distillations were carried out under an argon atmosphere. Elemental analyses were performed by Atlantic Microlab, Inc., Atlanta, GA. Tetra-n-butylammonium hexafluorophosphate (TBAF, Aldrich) was recrystallized from ethyl acetate and dried in vacuo.

Instrumentation. NMR spectra were recorded on either a 90-MHz JEOL FX90Q or a 300-MHz General Electric QE-300 spectrometer. ^{1}H NMR chemical shifts are reported in ppm downfield from an internal TMS standard, and the ^{13}C NMR chemical shifts are reported in ppm relative to the central resonance of the solvent as reference. Gas chromatographic analyses were performed on a Hewlett-Packard 5890 chromatograph. GC–MS measurements were carried out on a Hewlett-Packard 5890A chromatograph interfaced with a HP5970 mass spectrometer operating at 70 eV. UV–vis spectra were recorded on a Hewlett-Packard 8450A diode-array spectrometer with 2-nm resolution. All measurements were carried out with 10-mm quartz cells equipped with greaseless Teflon stopcocks. Infrared spectra were measured on a Nicolet 10DX FTIR spectrometer. Photochemical irradiations were performed with the focused beam from either a 500-W Osram high-pressure Hg or a 1-kW Hanovia Hg–Xe lamp. Corning sharp-cutoff filters CS3-68, CS3-70, and CS3-67 were used to absorb high-energy radiation at wavelengths (520, 500, and 550 nm) less than those of the charge-transfer bands.

Determination of the Formation Constants of the EDA Complexes. The toluene or CH$_2$Cl$_2$ (4 mL) solution of Cp$_2$MH$_2$ (0.02–0.03 g) was transferred to a quartz tube (1-cm pathlength) under an argon atmosphere. The UV–vis spectrum was measured with a sample of pure solvents as reference. Incremental amounts (2 equiv) of the organic acceptor were carefully added under a counterflow of argon. The absorbance was measured at two wavelengths close to λ_{max} of the CT band. The procedure was repeated to give at least six points under conditions where the concentration of organic acceptors was always greater than that of Cp$_2$MH$_2$.

Preparation of (C$_5$H$_5$)$_2$W(CHCNCHCN) (II). To a toluene (7 mL) solution of Cp$_2$WH$_2$ (0.1 g, 0.32 mmol) was added fumaronitrile (0.29 g, 3.79 mmol) portionwise. The red-orange solution was photolyzed with light at wavelengths greater than 550 nm for 62 h, with use of a 500-W mercury lamp and Corning (CS3-67) glass cutoff filter. The resulting pale red solution was decanted from the red crystalline solid, which was then washed with toluene and dried in vacuo: yield 0.047 g, 38%; mp 212–214 °C. ^{1}H NMR (DMSO-d_6): δ 4.96, 4.90, 4.86 (10 H, Cp), 1.74, 1.68 (2 H). The resonances at δ 4.96, 4.90, and 4.86 occurred in a 3:1:1

(56) Brintzinger, H. H.; Lohr, L. L., Jr.; Wong, K. L. T. *J. Am. Chem. Soc.* **1975**, *97*, 5146. See also discussion in ref 38.

(57) The neutral donors are assumed to have comparable energies.

(58) On the basis of the difference in bond dissociation energy[59] and E°_{ox}[20] for Cp$_2$MoH$_2$ and Cp$_2$MoH$_2^{\bullet+}$, a thermochemical (cycle) calculation indicates that Cp$_2$MoH$_2^{\bullet+}$ is more acidic than Cp$_2$WH$_2^{\bullet+}$ by $2.3RT(\Delta pK_a)$ = 16 kcal mol^{-1}.

(59) Calado, J. C. G.; Dias, A. R.; Simoes, J. A. M.; DaSilva, M. A. V. R. *J. Organomet. Chem.* **1979**, *174*, 77.

(60) Ko, J. J. Unpublished results.

(61) For a discussion of solvation differences in vertical and adiabatic ion pairs, see: Kochi, J. K. *Angew. Chem., Int. Ed. Engl.* **1988**, *27*, 1227.

(62) Compare: Hammond, G. S. *J. Am. Chem. Soc.* **1955**, *77*, 334.

(63) (a) Green, M. L. H.; McCleverty, J. A.; Pratt, L.; Wilkinson, G. *J. Chem. Soc.* **1961**, 4854. (b) Green, M. L. H.; Pratt, L.; Wilkinson, G. *J. Chem. Soc.* **1958**, 3916. (c) See also: King, R. B. *Organometallic Synthesis*; Academic: New York, 1965, Vol. 1, pp 79–81.

intensity ratio arising from equivalent Cp rings in the fumaronitrile adduct and inequivalent Cp rings in the maleonitrile isomer. The high-field resonances at δ 1.74 and 1.68 in a 3:2 intensity ratio were assigned to the fumaronitrile and maleonitrile ligands, respectively.[64] $^{13}C\{^1H\}$ NMR (DMSO-d_6): δ 112.9, 112.1 (CN), 7.5, 76.9, 75.7 (Cp), -7.74, -8.23 (CHCN). Since the ^{13}C resonances at δ 78.5, 76.9, and 75.7 occurred in a 1:3:1 intensity ratio, the first and third were assigned to the inequivalent Cp ligands in the maleonitrile adduct (compare above). The pair of high-field resonances at δ -7.74 and -8.23 were assigned to the fumaronitrile and maleonitrile ligands, respectively. Note that the cyano resonances at δ 112.9 and 112.1 were comparable to those in the free ligands.[65] IR (NaCl-Nujol): 2193 (s), 1307 (w), 1265 (m), 1166 (w), 1131 (w), 1110 (m), 1096 (w), 1019 (m), 998 (w), 934 (m), 920 (m), 885 (w), 836 (m), 801 (m), 732 (w) cm^{-1}. Anal. Calcd for $C_{14}H_{12}N_2W$: C, 42.88; H, 3.09; N, 7.14. Found: C, 42.97; H, 3.09; N, 7.19. The quantification of succinonitrile was carried out as follows. The decanted supernatant was treated with O_2 to destroy the unreacted Cp_2WH_2, whereupon the orange solution was bleached and a black solid precipitated. The resulting colorless solution was filtered on the silica gel pad and washed with $CHCl_3$ (50 mL). The volume of the colorless solution was carefully reduced in vacuo to approximately 4 mL for GC–MS analysis: found succinonitrile 0.11 mmol, 92% based on II; mass spectral cracking pattern of succinonitrile m/z (%) 81 (0.85), 80 (16), 79 (35), 54 (0.96), 53 (100), 52 (30), 51 (22). The supernatant was chromatographed on a column of silica gel with $CHCl_3$ as the eluent. The ^1H NMR spectrum of the waxy solid was identical with that of the authentic compound: R_f 0.18; yield 80%.

Preparation of $Cp_2WC_4H_2O_3$ (IV). To a toluene (8 mL) solution of Cp_2WH_2 (0.078 g, 0.25 mmol) was added maleic anhydride (0.242 g, 2.5 mmol) portionwise under argon. The resulting light greenish blue solution was irradiated for 58 h with the aid of the 550-nm cutoff filter. A light brown solid was formed slowly and periodically removed by centrifugation in order to maintain a clean light path. The resulting pale green solution was decanted from the pale brown solid, which was then recrystallized from CH_3CN: yield of IV 0.022 g (22%); mp 135–138 °C. ^1H NMR (DMSO-d_6): δ 5.06 (5 H, Cp), 4.70 (5 H, Cp), 3.05 (2 H). The resonances at δ 5.06 and 4.70 in a 1:1 intensity ratio were assigned to the inequivalent Cp ligands arising from the magnetic anisotropy of the cyclic anhydride functionality.[66] The ligand resonances at δ 3.05 was shifted upfield relative to that of the free ligand (δ 5.5).[67] $^{13}C\{^1H\}$ NMR (DMSO-d_6): δ 76.66, 75.96 (C_5H_5), 15.12 (W–C). The pair of resonances at δ 76.66 and 75.96 were assigned to the inequivalent Cp ligands, and the high-field resonance at δ 15.12 was attributed to the carbon bonded to the tungsten center. IR (NaCl-Nujol): 1781 (s), 1732 (sh), 1717 (s), 1231 (m), 1105 (w), 1068 (w), 1020 (w), 990 (w), 934 (m), 894 (s), 856 (w), 834 (w), 823 (w), 815 (m), 749 (w), 727 (w), 686 (m), 667 (w), 634 (m) cm^{-1}. Anal. Calcd for $C_{14}H_{12}O_3W$: C, 40.81; H, 2.95. Found: C, 41.47; H, 3.00. The quantification of succinic anhydride was carried out as follows. The decanted supernatant was treated with O_2 and the colorless solution filtered on a silica gel pad (3 cm) and washed with $CHCl_3$ (50 mL). The solution was carefully reduced in volume to ca. 5 mL. GC–MS analysis indicated the presence of succinic anhydride: 0.05 mmol (95%); mass spectrum m/z (%) 100 (0.08), 57 (3.12), 56 (100), 44 (7.75).

Preparation of $Cp_2Mo(CHCNCH_2CN)H$ (I). To a toluene (4 mL) solution of Cp_2MoH_2 (0.038 g, 0.17 mmol) was added fumaronitrile (0.156 g, 2.04 mmol) in 2-equiv quantities under an argon atmosphere. The resulting orange solution was irradiated for 3 h with the use of the 550-nm cutoff filter, whereupon an orange crystalline precipitate formed rapidly. The pale yellow supernatant was decanted from the orange crystals, and the crystals were washed with toluene and then dried in vacuo: yield

Table IV. Selected Bond Lengths (Å) in $Cp_2Mo(CHCNCH_2CN)H$ (I)

Mo–C(Cp)	2.237 (8)–2.358 (9)	C–C(Cp)	1.434 (9)–1.332 (10)
Mo–C(11)	2.287 (5)	C(11)–C(12)	1.559 (9)
Mo–H	1.529	C(11)–C(13)	1.446 (9)
N(1)–C(13)	1.127 (8)	C(12)–C(14)	1.456 (8)
N(2)–C(14)	1.120 (8)		

Table V. Selected Bond Angles (deg) in $Cp_2Mo(CHCNCH_2CN)H$ (I)

C(2)–Mo–C(11)	94.2 (2)	C(1)–Mo–C(11)	76.6 (2)
C(4)–Mo–C(11)	131.6 (2)	C(3)–Mo–C(11)	130.7 (2)
C(6)–Mo–C(11)	138.4 (3)	C(5)–Mo–C(11)	96.5 (2)
C(8)–Mo–C(11)	80.9 (2)	C(7)–Mo–C(11)	110.8 (3)
C(10)–Mo–C(11)	118.4 (2)	C(9)–Mo–C(11)	83.5 (2)
C(2)–Mo–H(M)	123.0 (2)	C(1)–Mo–H(M)	89.3 (2)
C(4)–Mo–H(M)	84.6 (2)	C(3)–Mo–H(M)	119.8 (2)
C(6)–Mo–H(M)	113.5 (2)	C(5)–Mo–H(M)	66.8 (2)
C(8)–Mo–H(M)	116.8 (2)	C(7)–Mo–H(M)	136.2 (3)
C(10)–Mo–H(M)	81.1 (2)	C(9)–Mo–H(M)	83.2 (2)
		C(11)–Mo–H(M)	77.6 (1)

0.049 g, 95%; mp 160–162 °C. ^1H NMR (DMSO-d_6): δ 5.02 (10 H, Cp), 2.49 (1 H, $J_{1,3}$ = 11.8 Hz, $J_{2,3}$ = 17.1 Hz), 2.40 (1 H, $J_{1,2}$ = 4.40 Hz), 1.91 (dd, 1 H, $J_{1,2}$ = 4.40 Hz, $J_{1,3}$ = 11.8 Hz), -8.56 (1 H). The alkyl protons (H_α, H_β, H_γ) gave second-order multiplets (ABX splitting) at δ 1.91, 2.40, and 2.49, which were computer-simulated to yield $J_{\alpha,\beta}$, $J_{\alpha,\gamma}$, and $J_{\beta,\gamma}$ similar to those observed in $Co(CN)_5(CH(CO_2Me)CH_2CO_2Me)$.[68] $^{13}C\{^1H\}$ NMR (DMSO-d_6): δ 130.41, 120.66 (CN), 85.63, 85.48 (Cp), 26.04 (CH$_2$CN), -12.85 (Mo–C). The diastereotopic Cp ligands were associated with the resonances at δ 85.6 and 85.5 and the carbon centers in the alkyl ligand with the resonances at δ -12.85 (bonded to M) and 26.04 (terminal). IR (Nujol–NaCl): 2233 (m), 2188 (s), 1839 (s),[69] 1275 (w), 1209 (w), 1168 (w), 1108 (w), 993 (m), 956 (w), 938 (w), 886 (w), 841 (m), 782 (s), 722 (m), 667 (m) cm^{-1}. Anal. Calcd for $C_{14}H_{14}N_2Mo$: C, 54.91; H, 4.61; N, 9.15. Found: C, 54.88; H, 4.62; N, 9.20.

Preparation of $Cp_2MoC_4H_2O_3$ (V). Maleic anhydride (0.36 g, 3.67 mmol) was added to a solution of Cp_2MoH_2 (0.105 g, 0.46 mmol) in toluene (8 mL) to give a light brown solution. Photolysis of this solution with use of a 500-W lamp and a 550-nm glass cutoff filter for 11 h yielded a light brown precipitate and a light green solution. The solution was removed by decantation. The residual light brown solid was recrystallized from CH_3CN: yield 0.064 g, 43%; mp 143–146 °C. ^1H NMR (DMSO-d_6): δ 5.12 (5 H, Cp), 4.77 (5 H, Cp), 3.08 (2 H). $^{13}C\{^1H\}$ NMR (DMSO-d_6): δ 80.08, 79.53 (Cp), 25.25 (Mo–C). IR (NaCl–Nujol): 1782 (s), 1729 (sh), 1715 (s), 1233 (m), 1107 (w), 1068 (w), 1022 (w), 994 (w), 938 (w), 889 (s), 850 (w), 834 (w), 804 (m), 749 (w), 727 (w), 692 (m), 625 (m) cm^{-1}. Anal. Calcd for $C_{14}H_{12}O_3Mo$: C, 51.68; H, 3.70. Found: C, 51.60; H, 3.75.

Thermal Decomposition Reaction of I. (a) The sealed NMR tube containing I (0.04 mmol) and fumaronitrile (0.24 mmol) was heated at 95–98 °C for $1^1/_2$ h. ^1H NMR (DMSO-d_6): δ 7.02 (fumaronitrile), 6.86 (maleonitrile) 4.91, 4.86 (10 H, Cp), 2.91 (succinonitrile), 2.06, 1.99 (2 H, CH). $^{13}C\{^1H\}$ NMR (DMSO-d_6): δ 116.30 (CN), 80.35, 77.80 (Cp), -4.05 (Mo–H).

(b) The sealed NMR tube containing I (0.065 mmol) and PEt_3 (0.32 mmol) in DMSO-d_6 was heated to 95–98 °C for 15 min. ^1H NMR: δ 3.86 (d, J_{HP} = 3.91 Hz), 2.91 (succinonitrile).

(c) The NMR tube containing I (0.06 mmol) and CCl_4 (0.30 mmol) in DMSO-d_6 was sealed and the tube warmed to room temperature. The ^1H NMR spectrum of the solution showed that the hydride band at δ -8.56 was completely missing. ^1H NMR (DMSO-d_6): δ 7.24 (CHCl$_3$), 6.11, 6.07 (10 H, Cp), 4.63–4.52 (m, 2 H), 4.49 (dd, 1 H).

X-ray Crystallography of the Hydrido Alkyl Adduct I of Cp_2MoH_2. A dark orange, diamond-shaped lozenge having approximate dimensions 0.26 × 0.48 × 0.48 mm was mounted on a glass fiber in a random orientation on a Nicolet R3m/V auto-

(64) Compare: (a) Fraser, M. S.; Baddley, W. H. *J. Organomet. Chem.* **1972**, *36*, 377. (b) Thomas, J. L. In ref 54.

(65) Tolman, C. A.; English, A. D.; Manzer, L. E. *Inorg. Chem.* **1975**, *14*, 2353.

(66) Bovey, F. A. *Nuclear Magnetic Resonance Spectroscopy*; Academic: New York, 1969; p 114.

(67) Compare also: (a) Yoshida, T.; Otsuka, S. *J. Am. Chem. Soc.* **1977**, *99*, 2134. (b) Tolman, C. A.; Seidel, W. C. *J. Am. Chem. Soc.* **1974**, *96*, 2774. (c) Weiss, E.; Stark, K.; Lancaster, J. E.; Murdoch, H. D. *Helv. Chim. Acta* **1963**, *46*, 288. (d) Tolman, C. A.; et al. In ref 65.

(68) Jackman, L. M.; Hamilton, J. A.; Lawlor, J. M. *J. Am. Chem. Soc.* **1968**, *90*, 1914.

(69) Compare: Fritz, H. P.; Hristidu, Y.; Hummel, H.; Schneider, R. Z. *Naturforsch., B* **1960**, *15*, 419.

Table VI. Atomic Coordinates ($\times 10^4$) and Equivalent Isotropic Displacement Parameters ($\text{Å}^2 \times 10^3$) for Cp$_2$Mo(CHCNCH$_2$CN)H (I)

	x	y	z	$U(\text{eq})^a$
Mo	1490 (1)	2300	8045 (1)	30 (1)
N(1)	-1895 (8)	2585 (5)	2710 (6)	56 (3)
N(2)	-5444 (9)	4785 (7)	3882 (9)	74 (3)
C(1)	2010 (9)	3953 (6)	6361 (9)	50 (3)
C(2)	2702 (10)	4359 (7)	8173 (10)	62 (3)
C(3)	4123 (9)	3450 (8)	9233 (10)	67 (3)
C(4)	4283 (9)	2567 (7)	8079 (10)	62 (4)
C(5)	2972 (10)	2866 (7)	6310 (11)	64 (4)
C(6)	2920 (10)	1362 (8)	10865 (9)	63 (3)
C(7)	1677 (11)	2187 (12)	10929 (8)	64 (3)
C(8)	-75 (11)	1935 (7)	9758 (9)	59 (3)
C(9)	-17 (10)	801 (7)	8859 (8)	55 (3)
C(10)	1875 (11)	418 (6)	9578 (9)	57 (3)
C(11)	-1436 (7)	2864 (5)	5960 (7)	38 (2)
C(12)	-2097 (9)	4242 (6)	6201 (8)	52 (3)
C(13)	-1691 (8)	2702 (5)	4135 (7)	41 (2)
C(14)	-3992 (9)	4553 (7)	4903 (10)	51 (3)

^{a} Equivalent isotropic U defined as one-third of the trace of the orthogonalized U_{ij} tensor.

matic diffractometer. The radiation used was Mo Kα monochromatized by a highly ordered graphite crystal. Final cell constants, as well as other information pertinent to data collection and refinement, are as follows: space group $P2_1$ (monoclinic); cell constants $a = 8.090$ (3) Å, $b = 10.282$ (4)Å, $c = 8.316$ (3) Å, $\beta = 116.92$ (3)°, $V = 617$ Å^3; molecular formula C$_{14}$H$_{14}$N$_2$Mo; formula weight 306.24; formula units per cell $Z = 2$; density $\rho = 1.65$ g cm^{-3}; absorption coefficient $\mu = 10.2$ cm^{-1}; radiation (Mo Kα) $\lambda = 0.710\,73$ Å; collection range $4° < 2\theta < 60°$; scan width $\Delta\theta = 1.70 + (\text{K}\alpha_2 - \text{K}\alpha_1)°$; scan speed range 2.0–15.0° min^{-1}; total data collected 1900; independent data with $I > 3\sigma(I)$ 1802; total variables 154; $R = \sum||F_o| - |F_c||/\sum|F_o| = 0.028$; $R_w = [\sum w(|F_o| - |F_c|)^2/\sum w|F_o|^2]^{1/2} = 0.028$; weights $w = \sigma(F)^{-2}$. The Laue symmetry was determined to be $2/m$, and from the systematic absences noted the space group was shown to be either $P2_1$ or $P2_1/m$. Intensities were measured with use of the $\theta/2\theta$ scan technique, with the scan rate depending on the count obtained in rapid prescans of each reflection. The internal quality of the sample was extremely poor, and thus, substantially wider than normal scan widths had to be used in order to ensure uniform backgrounds. Two standard reflections were monitored after every 2 h or every 100 data collected, and these showed no significant decay. In reduction of the data, Lorentz and polarization corrections were applied; however, no correction for absorption was made due to the small absorption coefficient and regular crystal shape. Since the molecule should not reasonably occupy a symmetry site, space group $P2_1$ was assumed from the outset. The structure was solved by interpretation of the Patterson map, which revealed the position of the Mo atom. The remaining non-hydrogen atoms were located in subsequent difference Fourier syntheses. The usual sequence of isotropic and anisotropic refinement was followed, after which all hydrogens attached to carbon were entered in ideal calculated positions and constrained to riding motion, with a single variable isotropic temperature factor. The hydride attached to Mo was located in a difference map but was found to wander to an unreasonable location when

allowed to refine independently. Therefore, in the final cycles of refinement the hydride was held fixed at the originally found coordinates. Since the compound crystallizes in a chiral space group, the Rogers test[31] was performed in order to determine the correct absolute configuration. This test indicated conclusively that the reported configuration is preferred over its inverse. After all shift/esd ratios were less than 0.1, convergence was reached at the agreement factors listed above. No unusually high correlations were noted between any of the variables in the last cycle of full-matrix least-squares refinement, and the final difference density map showed a maximum peak of about 0.6 e/Å^3. All calculations were made with use of Nicolet's SHELXTL PLUS (1987) series of crystallographic programs.

Reversible Oxidation Potentials of Cp$_2$MH$_2$ (M = Mo, W). The conventional cyclic voltammetry at scan rates $v < 10$ V s^{-1} and preparative-scale electrolysis were carried out as described previously.[70] Fast-scan cyclic voltammetry at $v > 200$ V s^{-1} employed a 5-μm (radius) Pt wire (Goodfellows, London) sealed in soft glass and polished to a mirror finish. Electrode connections were made with conductive paint (Nickel Print, GE Electronics). The three-electrode potentiostat was constructed locally and employed fast-response Motorola LF-357 operational amplifiers.[71] The voltage follower circuit was mounted external to the potentiostat to minimize the length of the wire from the working electrode and thus ensure low noise pickup. The potentiostat was driven by a Princeton Applied Research Model 175 universal programmer or Exact Model 628 function generator. Current and voltage signals were transferred to a Gould Biomation 4500 digital oscilloscope with 8-bit resolution and 10-ns response time. The interface to a Compaq Deskpro PC Model 3 computer allowed all further data manipulation (including subtraction of the charging current). All fast-scan cyclic voltammograms were performed in a Faraday cage to minimize 60-Hz interference. Voltages are reported relative to a saturated KCl–SCE reference electrode.

Freshly sublimed Cp$_2$MoH$_2$ and Cp$_2$WH$_2$ were made up in an inert-atmosphere box as either a 5×10^{-3} M (conventional CV) or 1×10^{-2} M (fast-scan CV) solution in acetonitrile containing 0.1 M TBAF. At conventional scan rates of $v < 10$ V s^{-1}, the cathodic wave on the initial positive scan of both Cp$_2$MoH$_2$ and Cp$_2$WH$_2$ was absent. At the fast-scan CV rates, the background charging current was first examined in the absence of hydrido-metal, but digital subtraction was unnecessary to establish reliable values of $E_p{}^a$ and $E_p{}^c$ as shown by the cyclic voltammograms in Figure 4.

Supplementary Material Available: Tables of bond distances and angles for I (1 page); a table of structure factor amplitudes (7 pages). Ordering information is given on any current masthead page.

(70) Kuchynka, D. J.; Amatore, C.; Kochi, J. K. *Inorg. Chem.* **1986**, *25*, 4087.

(71) Howell, J. O.; Kuhr, W. G.; Ensman, R. E.; Wightman, R. M. *J. Electroanal. Chem. Interfacial Electrochem.* **1986**, *209*, 77.